THE JOURNAL OF PHYSICAL CHEMISTRY B

Article

pubs.acs.org/JPCB

Influence of a Flavan-3-ol Substituent on the Affinity of Anthocyanins (Pigments) toward Vinylcatechin Dimers and Proanthocyanidins (Copigments)

Frederico Nave,[†] Natércia F. Brás,[‡] Luís Cruz,[†] Natércia Teixeira,[†] Nuno Mateus,[†] Maria J. Ramos,[‡] Florent Di Meo,[∥] Patrick Trouillas,[∥] Olivier Dangles,[§] and Victor De Freitas*[,†]

[†]Centro de Investigação em Química and [‡]REQUIMTE, Departamento de Química, Faculdade de Ciências, Universidade do Porto, Rua do Campo Alegre, 687, 4169-007 Porto, Portugal

[§]Université d'Avignon et des Pays de Vaucluse, INRA, UMR408, F-84000 Avignon, France

[∥]LCSN-EA1069, Université de Limoges, 2 rue du Dr Marcland, 87025 Limoges, France

ABSTRACT: The aim of this study is to investigate interactions possibly taking place in red wine between three flavanols (copigments, CP), i.e., two epimeric vinylcatechin dimers (CP1 and CP2) and catechin dimer B3 (CP3), and a specific pigment resulting from the condensation between the main grape anthocyanin malvidin 3-*O*-glucoside (oenin) and catechin, catechin-(4→8)-oenin. By comparison with our previous work on oenin itself, the influence of the catechin moiety of the anthocyanin in the binding is established. The thermodynamic parameters show that both vinylcatechin dimers exhibit a higher affinity for catechin-(4→8)-oenin, in comparison with proanthocyanidin B3, as previously observed with oenin. However, the corresponding binding constants are weaker, probably due to steric hindrance in the anthocyanin brought by the flavanol nucleus. Consequently, catechin-(4→8)-oenin should be much less stabilized by copigmentation in hydroalcoholic solution than oenin. Quantum mechanics and molecular dynamics simulations are also performed to interpret the binding data, to specify the relative arrangement of the pigment and copigment molecules within the complexes, and to interpret their absorption properties in the visible range.

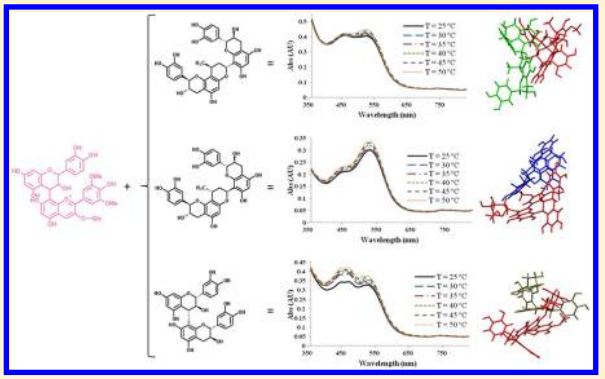

INTRODUCTION

Flavanol−anthocyanin adducts, such as catechin-(4→8)-oenin, result from the direct condensation between flavan-3-ols (catechin monomers and condensed tannins) and anthocyanins.[1,2] Such adducts, which were evidenced in wine[2,3] and fruit,[4−6] and their copigmentation complexes could contribute to the color of mature red wines, a point largely undocumented so far.

Although the anthocyanin moiety is obviously responsible for the color of flavanol−anthocyanin adducts, slight alterations (a λ_{max} blue shift of 8 nm) in the UV−visible spectrum can be attributed to the flavan-3-ol moiety.[7,8] In aqueous and hydroalcoholic solutions, as the pH is raised, the cationic flavylium form (AH^+, red) is very rapidly converted into neutral purple quinonoid bases (A, kinetic products) by deprotonation of one of the most acidic OH groups and more slowly into a colorless hemiketal (B, thermodynamic product, itself in equilibrium with small concentrations of *cis*- and *trans*-chalcones, C_c and C_t), by water addition onto the pyrylium ring of the residual red cation (Scheme 1). At mildly acidic pH, the colorless hemiketal is the dominant species.[9] This frame of structural transformations applies to all common anthocyanins. A previous work by some of the authors[9] has reported the thermodynamic and kinetic parameters of these reversible transformations for the flavanol−anthocyanin adduct [catechin-(4→8)-oenin] and has showed that the flavanol nucleus only marginally affects the anthocyanin behavior.

Despite the thermodynamic tendency of anthocyanins to form colorless hemiketals, natural colors expressed by anthocyanins are fairly stable. This evidences naturally occurring stabilization mechanisms, copigmentation being one of the most important. Copigmentation mainly refers to interactions between colorless phenols (copigments) and the planar polarizable nuclei of anthocyanins' colored forms.[10] The binding is promoted by the hydrophobic effects, mainly dispersive $\pi-\pi$ stacking interactions between the polarizable orbitals of the aromatic rings.[10−13]

Proanthocyanidins and vinylcatechin dimers (originated in wine by the cleavage of methylmethine-bridged flavan-3-ol oligomers and by the reaction between flavan-3-ols and acetaldehyde)[14] were shown to act as copigments.[12] In the present work, three of these copigments were tested for their

Received: August 6, 2012
Revised: October 17, 2012
Published: November 6, 2012

Scheme 1. Structural Transformations of Anthocyanins (e.g., cat-mv3glc) in Mildly Acidic Solution

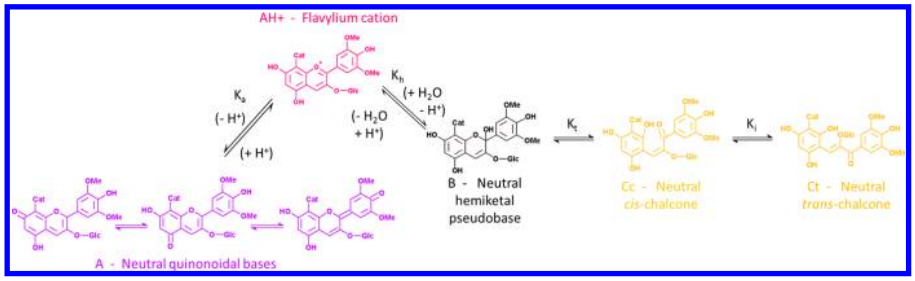

Scheme 2. Chemical Structures of the Pigment and the Copigments Investigated in This Work

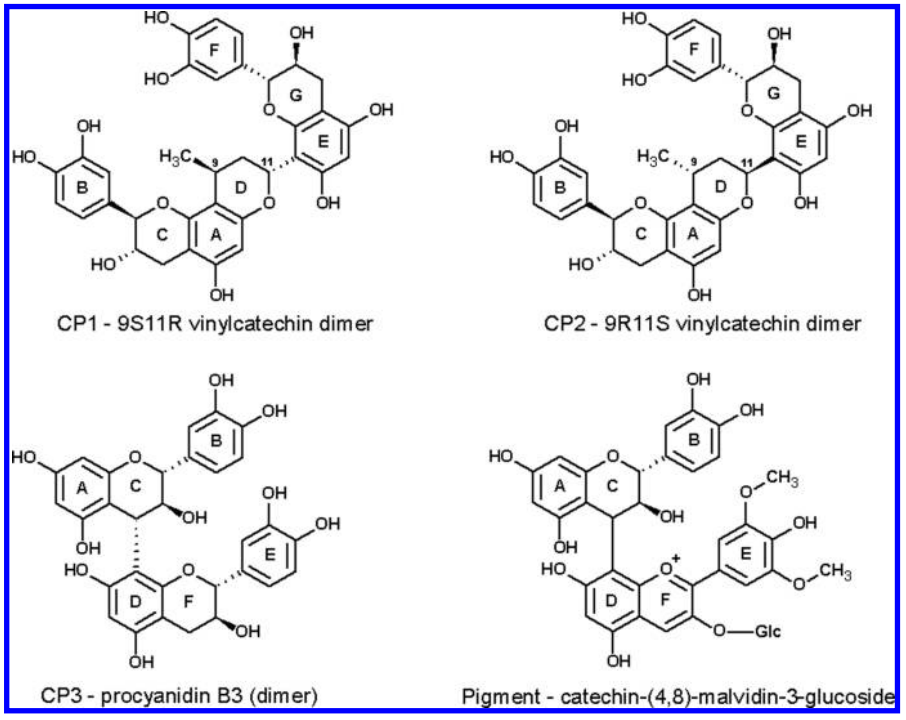

capacity to form complexes with catechin-(4→8)-oenin (Scheme 2). To the authors' knowledge, this is the first work dealing with the copigmentation of flavanol−anthocyanin adducts. A preliminary study on color loss (estimation of global hydration parameters) of catechin-(4→8)-oenin through experiments at variable temperature was carried out and compared to a previous more detailed investigation involving the stopped-flow technique.[9] Both studies provided consistent data. Similarity, copigmentation thermodynamic constants were estimated from the UV−visible spectra of the pigment + copigment mixtures recorded at different temperatures.

Finally, the consequences of the pigment/copigment on the visible spectrum of the pigment were also theoretically analyzed, thus providing a complete picture of the electronic transitions describing the excited states (involved in visible light absorption). The theoretical investigation includes a description of copigmentation for a prototype pigment/copigment pair, the optimal geometries of the three copigmentation complexes studied (evaluated by combining molecular dynamics and quantum calculations), and an analysis of the spectral shifts on the basis of time-dependent density functional theory (TD-DFT) calculations.

MATERIALS AND METHODS

Materials. Malvidin-3-*O*-glucoside (oenin) was extracted from a young red wine and purified by preparative chromatography, as described in previous reports.[15,16] Catechin-(4→8)-oenin was hemisynthesized as previously described.[15] Vinylcatechin epimeric dimers were synthesized according to a previous work.[14] Proanthocyanidin B3 was also hemisynthesized as described in the literature.[17] The purity of these compounds was assessed by HPLC and ^{1}H NMR.

UV/Vis Spectroscopy. A water−EtOH (9:1) mixture was used as the solvent throughout this work. A 0.2 M citrate buffer[12] was used to adjust the pH to 3.5. For flavylium hydration studies, a 0.1 M phosphate buffer[10] adjusted to pH 2.5 was also used. The ionic strength was adjusted to 0.5 M by addition of NaCl.

Spectroscopic measurements were performed on a Bio-Tek Power Wave XS spectrophotometer. Temperature effects on copigmentation and flavylium hydration were assessed at the following temperatures: 25, 30, 35, 40, 45, and 50 °C. The spectra were recorded between 360 and 830 nm (1 nm sampling interval) in a 1 cm path length cell.

Investigation of Flavylium Hydration. In a very acidic medium, with only the flavylium ion being present, the visible absorbance is

dx.doi.org/10.1021/jp307782y | J. Phys. Chem. B 2012, 116, 14089−14099

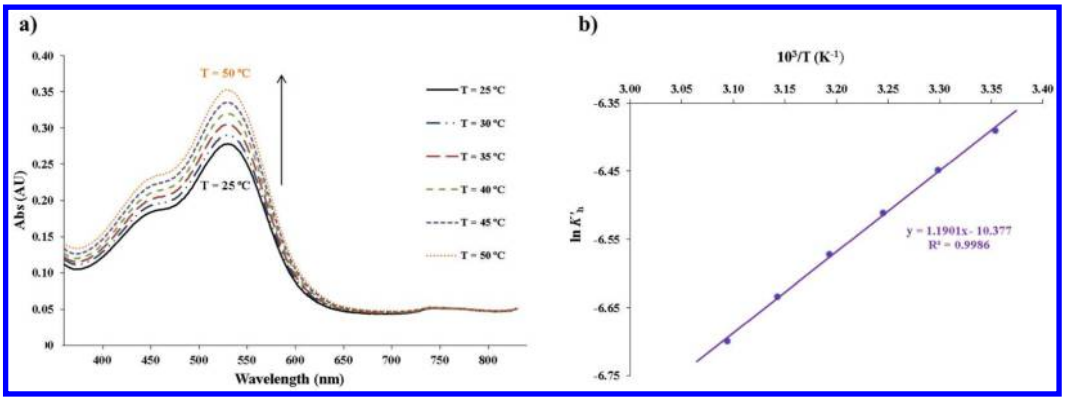

Figure 1. (a) Temperature dependence of the spectrum of catechin-(4→8)-oenin (10^{-4} M) in pH 3.5 citrate buffer containing 10% v/v EtOH. (b) Van't Hoff plot for the determination of the entropy and enthalpy changes of the overall hydration process of the catechin-(4→8)-oenin flavylium ion.

$$A_0 = \varepsilon_{AH^+} C$$

where C is the total pigment concentration. In a mildly acidic solution (pH 3.5, in our work) and neglecting the minor contribution of quinonoid bases, the visible absorbance becomes

$$A_0 = \varepsilon_{AH^+}[AH^+]$$

with

$$C = [AH^+] + [A] + [B] + [C_c] + [C_t]$$
$$= [AH^+] + [A] + [B']$$

where B′ is the pool of colorless forms in equilibrium.

Noting that K'_h is the *apparent* thermodynamic constant for the *overall* hydration process connecting the flavylium ion on the one hand and the pool of colorless forms on the other hand, we can write

$$K'_h = [H_3O^+]\frac{[B']}{[AH^+]} = K_h\{1 + K_t(1 + K_i)\}$$

where K_h is the thermodynamic constant of water addition on the flavylium ion, yielding hemiketal B; K_t is thermodynamic constant of cycle-chain tautomerization of B into *cis*-chalcone, C_c; and K_i is thermodynamic constant of isomerization of C_c into *trans*-chalcone, C_t.

For catechin-(4→8)-oenin, the K_t and K_i values are 0.13 and 0.15, respectively,[9] thus making the hemiketal by far the most abundant colorless form (>85%).

One can write

$$C = [AH^+]\left(1 + \frac{K_a + K'_h}{[H_3O^+]}\right) = [AH^+]\left(1 + \frac{K'_a}{[H_3O^+]}\right)$$

where $K'_a = K_a + K'_h \approx K'_h$

(see Nave et al.[9]).

From the equations above, one easily obtains

$$A = \frac{A_0}{1 + \frac{K'_h}{[H_3O^+]}}$$

From the latter equation, we can deduce

$$K'_h = 10^{-pH}\left(\frac{A_0}{A} - 1\right) \quad (1)$$

Equation 1 was used to estimate K'_h at different temperatures.[10] The entropy and enthalpy of the apparent hydration process were obtained from a linear Van't Hoff plot of ln K'_h vs $1/T$ (Figure 1). At each temperature, a 30 min equilibration period was imposed prior to measurement.

Copigmentation Studies. The copigmentation experiments were performed by adding aliquots of concentrated copigment (CP) solutions to a 0.1 mM catechin-(4,8)-oenin solution. In such dilute pigment solutions, anthocyanin self-association can be neglected.[13] After a 30 min period of equilibration, the UV−vis spectra were recorded. Each experiment was conducted in triplicate.

If we assume a 1:1 complexation stoichiometry,[10,12,18,19] the copigmentation binding constant (K_{CP}) is given by

$$K_{CP} = \frac{[AHCP^+]}{[AH^+][CP]}$$

The visible absorbance at pH 3.5 in the absence of copigment is

$$A_0 = \varepsilon_{AH^+}[AH^+] \quad \text{when} \quad C = [AH^+] + [B']$$

The visible absorbance at pH 3.5 in the presence of copigment is

$$A = \varepsilon_{AH^+}[AH^+] + \varepsilon_{AHCP^+}[AHCP^+] \quad \text{when}$$
$$C = [AH^+] + [B'] + [AHCP^+]$$

We thus have

$$A_0 = \frac{\varepsilon_{AH^+} C}{1 + \frac{K'_h}{[H_3O^+]}}$$

$$A = \frac{\varepsilon_{AH^+} C(1 + rK_{CP}[CP])}{1 + \frac{K'_h}{[H_3O^+]} + K_{CP}[CP]} \quad \text{where} \quad r = \frac{\varepsilon_{AHCP^+}}{\varepsilon_{AH^+}}$$

The free CP concentration, [CP], can be equated with the total CP concentration, $[CP]_t$, as the copigment/pigment molar ratio is high in all experiments (ca. 20).

By combining the latter two equations, K_{CP} can finally be expressed as[10,18,19]

$$K_{CP} = \frac{aH}{(ar - 1 - H)[CP]_t} \quad (2)$$

dx.doi.org/10.1021/jp307782y | J. Phys. Chem. B 2012, 116, 14089−14099

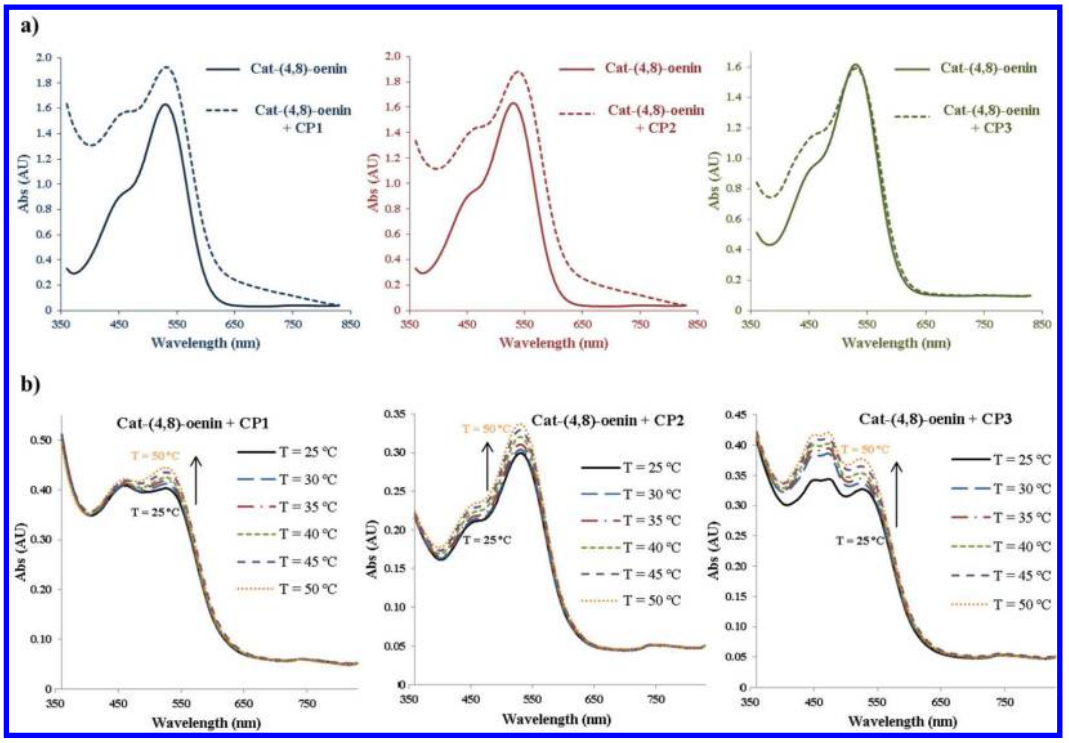

Figure 2. (a) Spectra of catechin-(4→8)-oenin (10^{-4} M) and catechin-(4→8)-oenin (10^{-4} M) + copigments (1:20) at very acidic pH (<1). From left to right: CP1 [(9*S*,11*R*)-vinylcatechin dimer], CP2 [(9*R*,11*S*)-vinylcatechin dimer], and CP3 (proanthocyanidin B3). (b) Temperature dependence of the spectra of catechin-(4→8)-oenin (10^{-4} M) + copigments (from left to right: CP1, CP2, and CP3) in a pH 3.5 citrate buffer containing 10% v/v EtOH.

where $a = 1 + K'_h/10^{-pH}$ and $H = (A - A_0)/A_0$ (relative absorbance amplification at the wavelength of the pigment's maximal absorption in the visible range, i.e., ca. 535 nm). Unlike common copigments (flavones and flavonols, hydroxycinnamic acids), none of the copigments investigated in this work induces a significant bathochromic shift in the flavylium ion's visible band (Figure 2a, pH <1, pigment under pure flavylium form). Only, a small increase of absorption, ca. 15%, is observed with CP1 and CP2 and attributed to possible light scattering due to the limited solubility of these copigments. Consequently, the *r* ratio is approximated to 1 throughout this work.

From eq 2, K_{CP} can be estimated at each temperature and the enthalpy and entropy of copigmentation can then be determined by a linear Van't Hoff plot of ln K_{CP} vs $1/T$.

Molecular Dynamics Simulations. The starting geometries of the copigment and pigment molecules were obtained at the HF/6-31G(d) level of calculation, using the Gaussian 09 package.[20] Atomic charges were further recalculated using the RESP procedure.[21] MD simulations were performed with GAFF (generalized amber force field) and the TIP3P model for the solute and water, respectively. Explicit solvation was included as a truncated octahedral box with a 12 Å distance between the box faces and any atom of the compound. Energy minimization occurred in two stages: first, the solute was kept fixed and only the position of the water molecules was optimized; second, the full system was optimized. Following a 100 ps equilibration procedure, 10 ns MD simulations were carried out. The Langevin thermostat was used,[22,23] and all the simulations were carried out in the *NPT* ensemble with periodic boundary conditions. All MD simulations were carried out using the Sander module, implemented in the Amber 10.0 simulations package,[24] with the Cornell force field.[25] Bond lengths involving H-atoms were constrained using the SHAKE algorithm,[26] and the equations of motion were integrated with a 2 fs time step using the Verlet leapfrog algorithm. Nonbonded interactions were truncated with a 12 Å cutoff. The temperature of the systems was maintained at 303.15 K.

Binding Free Energies. The MM_PBSA script (molecular mechanics−Poisson−Boltzmann surface area)[27−30] as implemented in Amber 10.0 was used to calculate the binding free energies ($\Delta G_{binding}$) for all complexes. A series of 120 geometries was extracted every 50 steps within the last 6000 ps of each simulation. The internal as well as the electrostatic and van der Waals interactions were calculated using the Cornell force field[25] with no cutoff. The electrostatic solvation free energy was calculated by solving the Poisson−Boltzmann equation with the software Delphi v.4.[31,32] The nonpolar contribution to the solvation free energy due to van der Waals interactions between the solute and the solvent and cavity formation was modeled as a term that is dependent on the solvent accessible surface area of the molecule. The relative binding energies ($\Delta\Delta G_{binding}$) were calculated with respect to the most stable complex.

Quantum Calculations for Complexation and Corresponding Optical Properties. Over the past decade, density functional theory (DFT) has been well-validated to evaluate conformational/electronic/optical properties of polyphenols. TD-DFT has appeared relevant to evaluate UV/vis absorption spectra of π-conjugated compounds. However, the choice of functionals is a determinant criterion to reach accuracy. In the present work long-range interaction is a key parameter. Classical DFT functionals fail in the description of (i) noncovalent interactions such as π-stacking interactions that are crucial in copigmentation complexes[33−38] and (ii) intra- and intermolecular charge transfer (CT) as observed in excited

dx.doi.org/10.1021/jp307782y | J. Phys. Chem. B 2012, 116, 14089−14099

states involving noncovalent interaction. New functionals have been recently developed to better describe the former point (noncovalent interaction) including DFT-D approaches (D meaning that dispersive contribution is taken into account in the formalism).[39−41] The latter point (intra- and inter-CT) is better described by range-separated hybrid (RSH) functionals, (e.g., ωB97).[42] As in the copigmentation complexes, both effects (π-stacking interactions and CT) are crucial, the classical hybrid functionals (e.g., PBE0 and B3P86), which usually provide accuracy for many single molecules, are not applicable here. The ωB97X-D functional hence appears relevant to correctly describe UV/vis absorption properties of copigmentation complexes at a reasonable computational time, regarding the size of the system.[43] [It was shown that ωB97X-D failed to exactly reproduce the absolute experimental wavelengths of polyphenols; however, in this case this is an appropriate method to allow an accurate (i) assignment of the different bands, (ii) description of the corresponding electronic transitions, and (iii) evaluation of the bathochromic shift attributed to copigmentation. For more details see Di Meo et al.[43]]

Due to the system size (mainly for complexes), the Pople-type double-ζ basis set 6-31+G(d) was chosen as a relevant compromise between accuracy and time demand.

The ground states (S_0) were optimized using ωB97X-D/6-31+G(d,p) from the average geometries of each complex as obtained from the MD simulations. Excited states were calculated within the TD-DFT formalism from S_0 geometries, thus providing the vertical transition, at the ωB97X-D/6-31G+(d,p) level of theory.

Quantum calculations were performed using the Gaussian 09 package.[20]

RESULTS AND DISCUSSION

Thermodynamics of Water Addition on the Flavylium Ion. For a quantitative interpretation of copigmentation in moderately acidic solution, the apparent hydration equilibrium must be taken into account. Indeed, the copigment interacts with the flat polarizable flavylium ion much more strongly than with the hemiketal. The resulting displacement of the hydration equilibrium toward the flavylium ion is responsible for the observed absorbance increase. In this work, the thermodynamics of water addition on catechin-(4→8)-oenin was briefly revisited to take into account differences in buffer composition and the influence of the EtOH cosolvent and compared with oenin itself.

The pK'_h values obtained for oenin (Table 1) are close to those previously published.[9,10,44,45] As already observed with malvin, the phosphate buffer tends to slightly decrease the pK_h value.[10] In agreement with a previous investigation,[9] the influence of the catechin moiety on the overall hydration equilibrium is very modest, as the pK_h difference between oenin and catechin-(4→8)-oenin is barely 0.1. By contrast, very significant differences are observed on the entropy and enthalpy changes. Indeed, whereas water addition on oenin is weakly endothermic or athermic with a moderately unfavorable entropy, water addition on catechin-(4,8)-oenin is exothermic with a largely unfavorable entropy. Indeed, when temperature is increased, hydration is favored with oenin and disfavored with catechin-(4,8)-oenin. It can be suggested that exothermic intramolecular interactions between the oenin and catechin moieties develop in the hemiketal, which would result in conformational restrictions.

Table 1. Thermodynamic Parameters of Water Addition for Oenin and Catechin-(4→8)-oenin in pH 3.5 Citrate Buffer

% EtOH	data	oenin	catechin-(4,8)-oenin
0	pK'_h (25 °C)	2.56	nd[a]
	ΔS_h^0 (J K^{-1} mol^{-1})	−34.5(±1.2)	nd
	ΔH_h^0 (kJ mol^{-1})	4.3(±0.4)	nd
	r^2	0.99	nd
10	pK'_h (25 °C)	2.64	2.73
	ΔS_h^0 (J K^{-1} mol^{-1})	ca. −50[b]	−86.1(±0.7)
	ΔH_h^0 (kJ mol^{-1})	ca. 0[c]	−10.1(±0.2)
	r^2	–	0.9992

[a]nd = not determined. [b]From $\Delta S_h^0 \approx R \ln K_h$, assuming athermic hydration ($\Delta H_h^0 \approx 0$). [c]K_h is essentially temperature-independent.

For both pigments, the presence of 10% EtOH only marginally affects the thermodynamics of flavylium hydration.

Thermodynamics of Copigmentation. Besides the typical absorbance increase, copigmentation is most frequently characterized by a bathochromic shift in the pigment's visible band.[10,18] That shift is best evidenced in strongly acidic solution in which the pigment is under a pure flavylium form (negligible hydration). Surprisingly, when the copigments were added to a strongly acidic solution of catechin-(4→8)-oenin (pH <1, copigment/pigment molar ratio = 20), no bathochromic shift is observed (Figure 2a).

At pH 3.5, each copigment (20 equiv) displays a different behavior in the presence of catechin-(4→8)-oenin. CP1 induces an additional band at 460 nm and increases the absorbance of the typical visible absorption band of the pigment (λ_{max} = 535 nm). CP2 increases the intensity of the pigment's visible band (with 450 nm shoulder growth being slightly more intense). Copigmentation by CP3 originates two new bands at 440 and 460 nm whose intensities are even stronger than that of the visible band at 535 nm (Figure 2).

In the copigmentation of anthocyanins by proanthocyanidins, the appearance of absorption bands at ca. 450 nm was previously reported and attributed to contamination by copigment oxidation products.[37]

By considering $r \approx 1$, eq 2 could be applied to estimate the values of K_{CP} from the absorbance signal at 535 nm at each temperature, and for each copigment, the enthalpy and entropy of copigmentation (Table 2) were obtained from a linear ln K_{CP} vs $1/T$ plot (Figure 3).

Table 2. Thermodynamic Parameters for the Copigmentation of Catechin-(4→8)-oenin by the Three Copigments

copigment	CP1	CP2	CP3
ΔS_{CP}^0 (J K^{-1} mol^{-1})	−12.0(±2.5)	−24.2(±4.1)	−69.2(±2.9)
ΔH_{CP}^0 (kJ mol^{-1})	−17.8(±0.8)	−22.7(±1.2)	−32.5(±0.9)
ΔG_{CP}^0 (kJ mol^{-1})	−14.2	−15.5	−11.9
ΔG_{CP}^0 (kcal mol^{-1})	−3.4	−3.7	−2.8
K_{CP} at 25 °C (M^{-1})	311	516	121
r^2	0.996	0.995	0.998

For all copigments, the complexation process is exothermic (negative ΔH_{CP}^0), in agreement with several previous studies.[10,38] The negative (unfavorable) entropy change suggests that the hydrophobic effect does not compensate the loss of rotational and translational freedom in the pigment and copigment molecules when they associate. The values of the

dx.doi.org/10.1021/jp307782y | J. Phys. Chem. B 2012, 116, 14089−14099

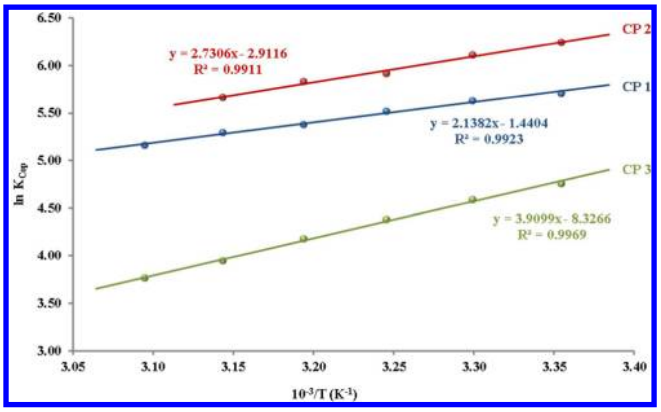

Figure 3. Van't Hoff plot for the determination of the entropy and enthalpy changes of copigmentation of the catechin-(4→8)-oenin by the copigments (1:20 molar ratio) in pH 3.5 citrate buffer containing 10% v/v EtOH.

binding constant and free enthalpy point to the following hierarchy in the overall affinity of the copigments for catechin-(4→8)-oenin: CP3 < CP1 < CP2. The same ranking was observed with oenin, but the corresponding binding constants (respectively, 351, 1927, and 5417 M^{-1}) were lower by a factor 3−10.[12] This difference can be explained by the higher steric hindrance caused by the additional flavanol (catechin) unit linked to the anthocyanin. CP2 emerges as a better ligand of catechin-(4→8)-oenin than CP1 owing to a more exothermic binding. Although even more exothermic, the binding of CP3 is weaker, probably because of a substantial conformational change in the flexible CP3 when it binds the pigment (e.g., restricted rotation about the 4,8 interflavanol bond leading to a more unfavorable entropy change).

The theoretical spectra of the pigment−copigment complexes can be constructed by assuming a negligible contribution of the quinonoid bases. From the copigmentation constant, the percentage of free AH^+ can be calculated and its spectral contribution subtracted from the experimental spectrum. The result is the spectrum of bound AH^+, i.e., the copigmentation complex. In the case of copigmentation with CP2, the binding was almost total, so the experimental spectrum only pertains to the copigmentation complex. The spectra of the complexes involving CP1 and CP3 present a new band in the range 440−460 nm. The spectrum of the complex involving CP2 presents the bands characteristic of catechin-(4→8)-oenin (450 and 535 nm). The new bands around 450 nm were explained as the result of copigmentation between CP1, CP3, and the flavylium ion of the catechin-(4→8)-oenin (see the theoretical investigation below). Copigmentation of the quinonoid bases (although minor at pH 3.5) could also make a contribution, as those forms are also prone to stacking interactions with copigments.[46,47] However, as the quinonoid bases and their copigmentation complexes absorb the visible light at higher wavelengths than their flavylium counterparts, no specific contribution in the range 440−460 nm is expected. Copigmentation of quinonoid bases also promotes a batho-chromic shift (which is not observed in our case), especially with purine copigments like caffeine and theophylline.[48]

Quantum Rationalization of a Prototype Pigment/Copigment System. Due to the size of the pigment/copigment system, we first proposed a full rationalization of copigmentation on a prototype system, namely, the catechin:3-*O*-methylmalvidin complex (Figure 4), smaller in size and thus easier to fully analyze at the quantum level. The entire potential energy surface was explored and three geometries were obtained (orientations 1, 2, and 3). In orientation 1, the two partners are parallel to each other, with the A- and C-rings of catechin interacting with the A-ring of malvidin (Figure 4a). The other two orientations are head-to-head, with the A-ring of catechin interacting with the C-ring of malvidin (orientation 2; see Figure 4b) or the A- and B-rings of catechin interacting with A- and B-rings of malvidin (orientation 3; see Figure 4c). The highest π-overlap is obtained for orientation 3. As usually observed in $\pi-\pi$ complexes, no strict cofacial (face-to-face) arrangement occurs but only the so-called parallel-displaced one (orientation 3) (Figure 4). The orientations exhibit considerable negative binding energies (Table 3) in which the dispersive contribution is high (ΔE^{disp} = −37.1, 38.4, and −42.5 kcal mol^{-1} for the three orientations, respectively). [Binding energies are expected to be overestimated since (i) the s_6 parameter of B3P86-D is not optimized, (ii) calculations have been performed in the gas phase, which probably leads to a significant overestimation of the stabilization attributed to intra-H bonding, and (iii) binding energies are compared to

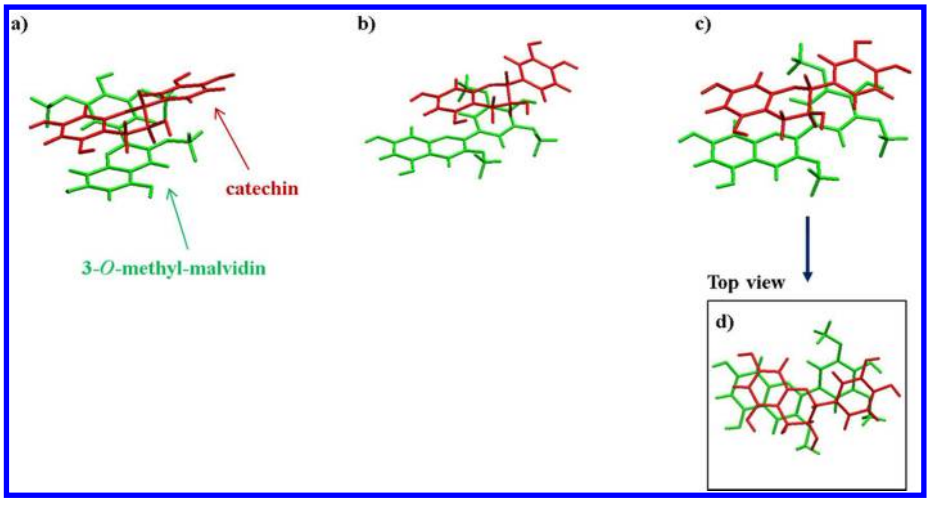

Figure 4. Optimized (B3P86-D/cc-pVDZ) geometries for the [catechin:3-*O*-methylmalvidin] prototype complex for the three more favorable orientations: (a) orientation 1, (b) orientation 2, and (c) orientation 3 (showing (d) parallel displaced stacking in a top view).

dx.doi.org/10.1021/jp307782y | *J. Phys. Chem. B* 2012, 116, 14089−14099

Table 3. Binding Energies (kcal mol^{-1}), Boltzmann Weights (D_{bolz}), and S$_0$ q^{CT} (e) Calculated for All the Most Stable Geometries of [Catechine:3-*O*-methylmalvidin] with B3P86-D (s_6 = 1.05)/cc-pVDZ

orientation	ΔE	ΔE^{disp}	D_{bolz} (%)	q^{CT}
1	−36.5	−37.1	55	0.08
2	−34.3	−38.4	2	0.13
3	−36.3	−42.5	43	0.11

experimental binding Gibbs energies, thus including entropic effects that cannot be calculated here. To tackle the second point, solvent effects should be taken into account not only implicitly but also explicitly, as inter-H bonding is probably crucial in aqueous solutions. Due to the size of the systems studied here, the corresponding calculations are not feasible.] π-Stacking appears definitely as the major contribution, whereas H-bonding is relatively weak since the distances are higher than 2.3 Å. The Boltzmann distribution is 55%, 2%, and 43% for the three conformers, respectively (Table 3). In these complexes, charge transfer (from catechin to malvidin) is possible in the ground state S$_0$ (q^{CT} = 0.08, 0.11, and 0.13 |e|, respectively).

For the three orientations, the classically described bathochromic shift attributed to copigmentation is observed (Table 4). The intensity of this shift is however very dependent on the

Table 4. Maximum Vertical Excitation Energies (E_{max}, eV), Absorption Wavelengths (λ_{max}, nm), Oscillator Strengths (f), MO Descriptions, Excitation Energy Shifts (ΔE_{max}, eV), and Absorption Wavelength Shifts ($\Delta\lambda_{max}$, nm)[a]

	orientation	E_{max}	λ_{max}	f	MO description
3-*O*-methylmalvidin		2.72	456.2	0.78	H→L (67%)
[catechin:3-*O*-methylmalvidin]	1	2.63	471.1	0.49	H→L (66%)
		3.10	400.1	0.05	H-1→L[b] (30%)
		3.23	383.6	0.08	H-1→L[b] (34%)
	2	2.63	471.2	0.43	H-1→L (52%)
		3.27	379.2	0.01	H→L[b] (55%)
	3	2.50	496.7	0.45	H→L (64%)
		2.76	448.7	0.01	H-1→L[b] (43%)

[a]The energy and wavelength shifts are calculated with respect to the 3-*O*-methylmalvidin. [b]Vertical transition is included in a more or less complex band involving more than one simple vertical transition.

orientation, −0.09 eV (14.9 nm), −0.09 eV (14.9 nm), and −0.22 eV (40.5 nm), for the three orientations, respectively. In this prototype copigmentation complex, the absorption maximum wavelength corresponds to the first excited state S$_1$, which is constituted of electronic transitions involving HOMO (highest occupied molecular orbital), HOMO-1, and LUMO (lowest unoccupied molecular orbital). LUMO is mainly localized on the entire malvidin moiety and, depending on the orientation, the distribution of HOMO and HOMO-1 may significantly differ. In orientation 1, HOMO is mainly localized on the malvidin moiety (as for LUMO), which allows an efficient MO (molecular orbital) overlap. In orientations 2 and 3, the HOMO is mainly localized on the B-ring of catechin. In this case, the contribution to the excited state of charge transfer (CT) from copigment to pigment increases and this is responsible of the bathochromic shift. Therefore, the electronic transitions are tuned by (i) MO overlap and the classical electronic transition contribution and (ii) CT, which may occur in the excited state. Both contributions are more or less important, depending on the orientation. Here it is possible to confirm, as previously shown for the flavanol−anthocyanidin copigment complex, that the optical properties must be rationalized after a careful analysis of the potential hypersurface. The spectral shifts are obtained by averaging over all the possible copigmentation complex geometries, according to the Boltzmann distribution.

Theoretical Conformations of the Three Pigment−Copigment Complexes. MD simulations allow sampling of the potential hypersurface so as to isolate several conformations for each copigmentation complex. The relative binding energies obtained by the MMPBSA procedure are in relatively good agreement with the experimental results (Table 5), which

Table 5. Differences in the Binding Free Energy Values ($\Delta\Delta G_{binding}$) of the Copigmentation Complexes

	$\Delta\Delta G_{binding}$ (kcal mol^{-1})	
complex	calcd (MM_PBSA)	exptl
[CP1:catechin-oenin]	7.48	0.31[a]
[CP2:catechin-oenin]	0	0
[CP3:catechin-oenin]	6.39	0.89[a]

[a]Experimental values calculated from Table 2 using $\Delta\Delta G = RT \ln(KCP2/KCPx)$.

confirms the relevancy of the MD procedure to provide an accurate picture for quantum analysis. [The results reveal that the $\Delta G_{binding}$ energy of the CP2:cat-mv3glc complex is the most negative one compared to the copigmentation complexes with CP1 and CP3. Although the tendency obtained for the binding free energies is CP2 > CP3 > CP1, the small difference in $\Delta\Delta G_{binding}$ between CP1 and CP3 (0.58 and 1.09 kcal mol^{-1}, experimental and theoretical values, respectively) is negligible and within the error range of the MM_PBSA calculations.] Indeed, for these copigmentation complexes it must be stressed that the exploration of the potential hypersurface is not feasible at the quantum level. Nonetheless, the interactions existing in these types of complexes must be treated by state-of-the-art methods. In particular, the description of H-bonding, π-stacking, and CT is highly dependent on the method. As noticed for the prototype system, the rationalization of optical properties strongly depends on the conformation. Hence, using a series of MD averaged geometries of complexes as starting geometries, DFT-D optimization was performed and allowed identifying three, three, and four geometries for the three complexes [CP1:catechin-(4→8)-oenin], [CP2:catechin-(4→8)-oenin], and [CP3:catechin-(4→8)-oenin], respectively (Figure 5).

Unlike the prototype system, the number of degrees of freedom is very large and steric hindrance does not allow optimized π-stacking arrangements. However, due to the numerous OH groups, H-bonding now plays a major role in the binding. Anyway, even if π-interactions are no longer the only driving force, they still take place in all complexes. In most conformers, the D- and F-rings of the pigment make π-type interactions with (i) C-, A-, and D-rings of CP1 and CP2 and (ii) C- and A-rings with CP3 (Table 6). Then depending on

dx.doi.org/10.1021/jp307782y | J. Phys. Chem. B 2012, 116, 14089−14099

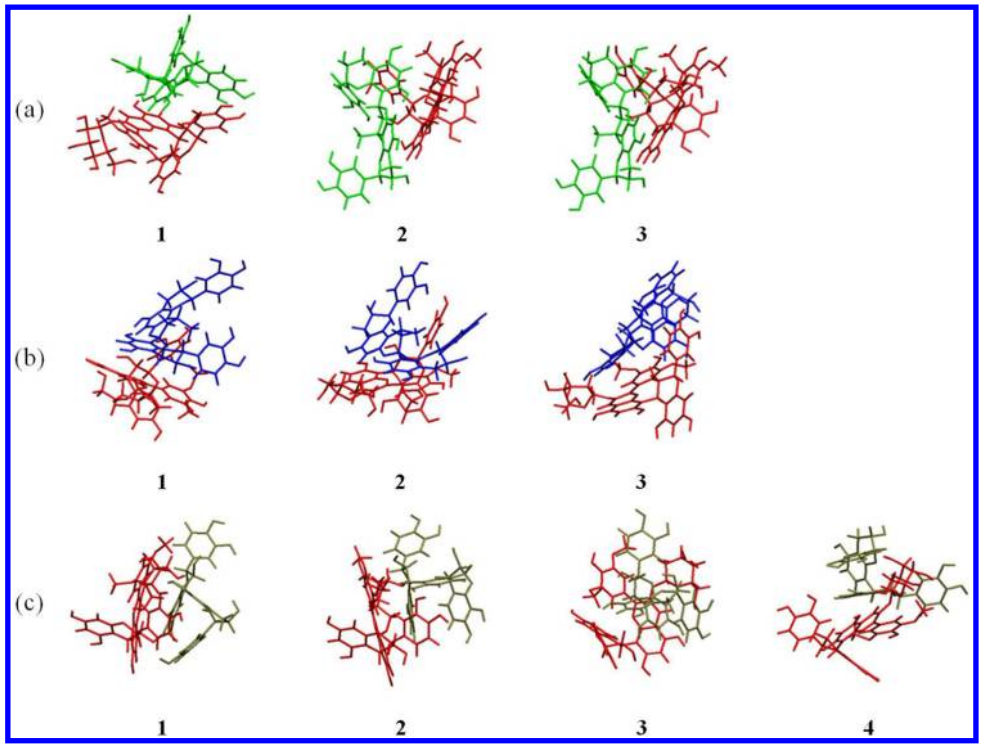

Figure 5. All optimized (B3P86-D/cc-pVDZ) geometries for (a) [CP1:catechin-(4→8)-oenin], (b) [CP2:catechin-(4→8)-oenin], and (c) [CP3:catechin-(4→8)-oenin] complexes. The pigment catechin-(4→8)-oenin is in red, and CP1, CP2 and CP3 are in green, blue, and brown, respectively.

Table 6. Geometrical Characteristics for Each Complex Obtained from the DFT-D Calculations

complex	orientation	pigment moiety[a]	copigment moiety[a]	minimal π-stacking distance (Å)	number of intermolecular H-bonds	average H-bond distance (Å)	ΔE^{CP} (kcal mol^{-1})
[CP1:cat-oenin]	1	DF	CAD	3.23	3	1.88	−57.6
		B	F	3.17			
	2	DF	CAD	3.41	3	1.87	−64.9
		B	F	3.23			
	3	DF	CAD	3.46	3	1.82	−50.1
		B	F	3.13			
[CP2:cat-oenin]	1	DF	GE	3.11	1	2.26	−24.1
		B	CAD	3.46			
	2	DF	CAD	3.45	3	2.21	−31.0
	3	DF	GE	3.93	5	1.92	−26.0
		B	CAD	3.21			
[CP3:cat-oenin]	1	DF	A	3.35	5	1.98	−46.0
		E	C	3.61			
	2	DF	A	3.24	3	2.02	−49.6
		E	C	3.88			
	3	DF	A	3.25	4	2.00	−41.6
	4	E	AC	3.21	1	1.85	−30.5

[a]Involved in π-stacking.

the complex, the B- or E-ring of the pigment interacts with the C-, A-, D-, and F-rings of the copigments (Table 6). All these interactions occur at a distance of around 3.5 Å, which is typically observed for π-stacking interactions. Again, no cofacial arrangement is observed, but as expected, parallel-displaced stacking occurs.

Classical Bathochromic Shift in Pigment−Copigment Complexes. As for the prototype, the visible absorption band is attributed to the first excited state S_1. However, the structure of S_1 is much more complex, which requires a careful analysis. The visible absorption band is basically constituted of electronic transitions from different MOs (HOMO, HOMO-1, HOMO-2, HOMO-3, HOMO-4, etc. down to even HOMO-10) to LUMO (Table 7). Again, the description of the excited state strongly depends on the conformer. In most cases a more or less pronounced bathochromic shift is observed. However, a hypsochromic shift is observed in one conformer (Table 7).

dx.doi.org/10.1021/jp307782y | J. Phys. Chem. B 2012, 116, 14089−14099

Table 7. Maximum Vertical Excitation Energies (E_{max}, eV), Absorption Wavelengths (λ_{max}, nm), Oscillator Strengths (f), MO Descriptions, Excitation Energy Shifts (ΔE_{max}, eV), and Absorption Wavelength Shifts ($\Delta\lambda_{max}$, nm) of the Different Complexes[a]

compound	conformer	E_{max}	λ_{max}	f	MO description	ΔE_{max}	$\Delta\lambda_{max}$
pigment		2.87	432.6	0.46	H-2→L (59%)	–	–
[CP1:cat-oenin]	1	2.74	453.3	0.25	H-2→L (47%) H→L (30%)	−0.13	20.6
	2	2.91	425.7	0.30	H→L (39%)	0.05	−6.9
	3	2.80	443.5	0.25	H-1→L (47%)	−0.07	10.8
[CP2:cat-oenin]	1	2.64	470.0	0.10	H-4→L (65%)	−0.23	37.4
	2	2.72	455.3	0.19	H-4→L (44%) H-3→L (38%)	−0.14	22.6
	3	2.76	449.3	0.35	H-10→L (42%)	−0.11	16.6
[CP3:cat-oenin]	1	2.63	470.7	0.09	H→L (45%)	−0.23	38.1
	2	2.67	463.6	0.20	H-2→L (45%)	−0.19	31.0
	3	2.78	445.4	0.19	H-2→L (60%)	−0.08	12.8
	4	2.62	473.0	0.31	H-2→L (51%)	−0.24	40.3

[a]The energy and wavelength shifts are calculated with respect to stand-alone pigment.

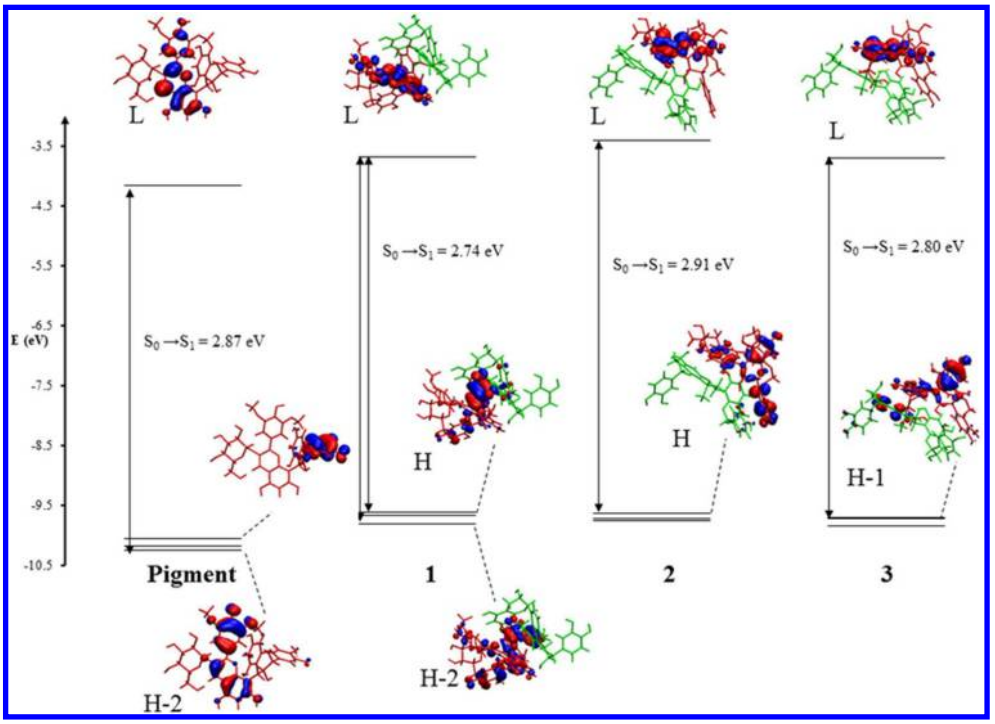

Figure 6. MO correlation diagram of pigment and conformers 1, 2, and 3 of the [CP1:catechin-(4→8)-oenin] copigmentation complex.

The [CP1:catechin-(4→8)-oenin] complex perfectly exemplifies the optical behavior of these complexes. In this case, the bathochromic shift is observed with conformers 1 and 3, whereas a hypsochromic shift is obtained with conformer 2 ($\Delta\lambda_{max}$ = 20.6, −6.9 and 10.8 nm for conformers 1, 2, and 3, respectively, see Table 7). The bathochromic shift is mainly attributed to the contribution of a CT excited state (see Figure 6), which occurs from the A-, C-, and D-rings of the copigment to the E-ring of the pigment, for both conformers 1 and 3. The CT allows a global stabilization of S_1, inducing a lower energy for the $S_0 \rightarrow S_1$ transition and a higher absorption wavelength (Table 7). For the conformer 2, no CT is observed in S_1, in agreement with the absence of bathochromic shift. Concomitant to the decrease in CT, the classical contribution to the transition may increase, thus increasing oscillator strengths (f = 0.30 for conformer 2).

The bathochromic shift in copigmentation complexes appears as a subtle effect, which is strongly influenced by the conformations and orientations of both pigment and copigment. At the quantum level, the sampling is not sufficient to exactly reproduce the experimental UV/vis spectra. [Quantum calculations are not able to reproduce experimental values because (i) calculations have been carried out in vacuo without taking solvent effects into account and (ii) the MD approach used to generate the starting geometries for QM calculations is not sufficient to allow the complete exploration of the potential energy surface (PES).] However, quantum calculations allow providing an accurate MO description of the visible absorption band. From the quantum calculations we can firmly conclude that the broadening of the experimental visible absorption band is not only attributed to solvent effects, as usual, but also comes from the presence of different conformers with different optical properties.

dx.doi.org/10.1021/jp307782y | J. Phys. Chem. B 2012, 116, 14089−14099

Rationalization of the New Bands in the 400−500 nm Range. The new bands observed for [CP1:catechin-(4→8)-oenin] and [CP3:catechin-(4→8)-oenin] are mainly attributed to excited states S_2 and/or S_3. Again, these excited states are complex, i.e., constituted of different electronic transitions from different MOs (from H-1 to H-11) but always to the LUMO. However, even if the description of S_2 and S_3 is complex, most of the electronic transitions involved in these two excited states exhibit a contribution of intramolecular CT within in the pigment. Such CT mainly occurs from the C- and A-rings of the catechin moiety to the malvidin moiety (as seen in Figure 7

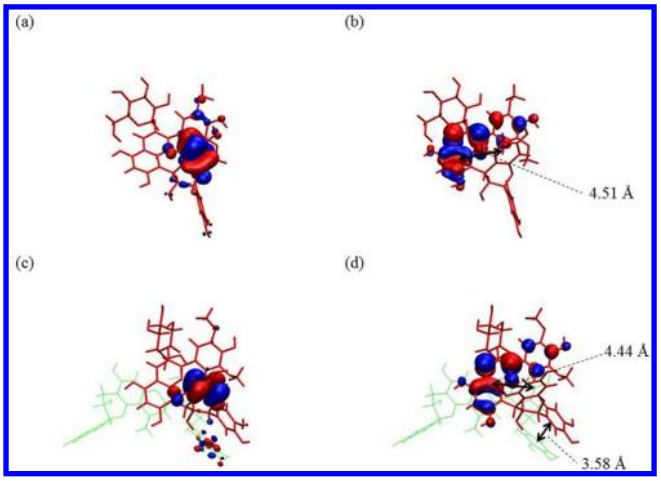

Figure 7. Spatial distribution of the MOs involved in the transition corresponding to the band ranging between 400 and 500 nm: (a) HOMO-3 and (b) LUMO of the pigment catechin-(4→8)-oenin in the absence of copigment and (c) HOMO-4 and (d) LUMO of conformer 3 of [CP1:catechin-(4→8)-oenin]. The pigment is in red while the copigment is in green. Here we can see that HOMO-3(4) and LUMO are on two separated moieties, so the corresponding transition requires CT.

for, e.g., conformer 3 of [CP1:catechin-(4→8)-oenin]). This intramolecular CT is definitely characteristic of the new band in the 400−500 nm range, which actually exists in the free pigment itself but only with very low oscillator strength. In the copigmentation complexes, this band can be amplified due to conformational changes in the pigment brought about by the copigment (Figure 7). This enhancement of CT within the pigment depends on the conformer and complex. In the case of [CP2:catechin-(4→8)-oenin], this effect is weak for most conformers while it is more important for [CP3:catechin-(4→8)-oenin] (Figure 8), in very good agreement with the experimental data (Figure 2b): for CP3, a double band arises around 440 nm, and for CP2 a single band arises at 450 nm amplifying the shoulder of the anthocyanic spectra at this wavelength.

CONCLUSION

This work has shown that the flavan-3-ol substituent of catechin-(4,8)-oenin weakens the affinity of the pigment for vinylcatechin dimers and proanthocyanidins because of steric constrains. In these copigmentation complexes, the driving force is a combination of π-stacking interactions and H-bonding. The theoretical investigation of the copigmentation complexes by a combination of molecular dynamics and DFT approaches has allowed valuable spatial representations of the complexes and a deep insight in the description of their

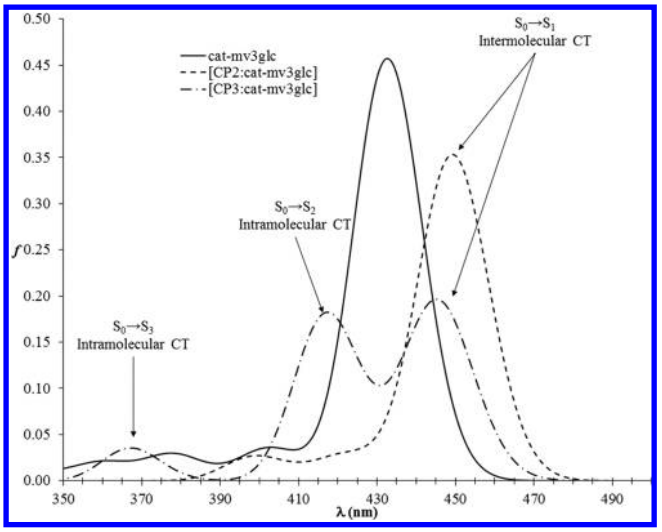

Figure 8. Theoretical UV/vis absorption spectra of catechin-(4→8)-oenin and both complexes [CP2: catechin-(4→8)-oenin] and [CP3: catechin-(4→8)-oenin]. The former complex exhibits the enhancing of the second and third absorption bands, corresponding to the S2 and S3 excited states. These bands are weaker (almost hidden) for the pigment itself and the latter complex. Note that the absorption wavelengths are shifted compared to the experimental spectra.

absorption properties in the visible range. The shift in the pigment's visible band brought about by the copigment appears strongly dependent on the copigment's structure and orientations of the two partners within the complex. Although bathochromism is usually observed, this effect can be canceled out by averaging over all the stable geometries. The quantum calculations have also succeeded in interpreting absorption bands in the 400−500 nm range, which are attributed to intramolecular CT within the pigment.

AUTHOR INFORMATION

Corresponding Author

*E-mail: vfreitas@fc.up.pt. Fax: +351.226082959. Tel: +351.226082862.

Notes

The authors declare no competing financial interest.

ACKNOWLEDGMENTS

The authors thank the "Conseil Régional du Limousin" for financial support and CALI (CAlcul en LImousin) for computing facilities. Research in Limoges is also supported by COST (FA1003 "East-West Collaboration for Grapevine Diversity Exploration and Mobilization of Adaptive Traits for Breeding" and CM0804 "Chemical Biology with Natural Compounds"). The authors (F. N., L.C., N.T., and N.F.B.) gratefully acknowledge the financial support of FCT - Fundação para a Ciência e Tecnologia through scholarships (SFRH/BD/30294/2006, SFRH/BPD/72652/2010, SFRH/BD/70053/2010 and SFRH/BD/31359/2006, respectively).

REFERENCES

(1) Salas, E.; Fulcrand, H.; Meudec, E.; Cheynier, V. *J. Agric. Food Chem.* **2003**, *51*, 7951−7961.

(2) Salas, E.; Atanasova, V.; Poncet-Legrand, C.; Meudec, E.; Mazauric, J. P.; Cheynier, V. *Anal. Chim. Acta* **2004**, *513*, 325−332.

(3) Vivar-Quintana, A. M.; Santos-Buelga, C.; Francia-Aricha, E.; Rivas-Gonzalo, J. C. *Food Sci. Technol. Int.* **1999**, *5*, 347−352.

(4) Fossen, T.; Rayyan, S.; Andersen, O. M. *Phytochemistry* **2004**, *65*, 1421−1428.
(5) Gonzalez-Paramas, A. M.; da Silva, F. L.; Martin-Lopez, P.; Macz-Pop, G.; Gonzalez-Manzano, S.; Alcalde-Eon, C.; Perez-Alonso, J. J.; Escribano-Bailon, M. T.; Rivas-Gonzalo, J. C.; Santos-Buelga, C. *Food Chem.* **2006**, *94*, 428−436.
(6) Gonzalez-Manzano, S.; Perez-Alonso, J. J.; Salinas-Moreno, Y.; Mateus, N.; Silva, A. M. S.; de Freitas, V.; Santos-Buelga, C. *J. Food Compos. Anal.* **2008**, *21*, 521−526.
(7) *Methods in Polyphenol Analysis*; Williamson, G., Santos-Buelga, C., Eds.; Royal Society of Chemistry: Cambridge, 2003.
(8) Salas, E.; Le Guerneve, C.; Fulcrand, H.; Poncet-Legrand, C.; Cheynier, W. *Tetrahedron Lett.* **2004**, *45*, 8725−8729.
(9) Nave, F.; Petrov, V.; Pina, F.; Teixeira, N.; Mateus, N.; de Freitas, V. *J. Phys. Chem. B* **2010**, *114*, 13487−13496.
(10) Galland, S.; Mora, N.; Abert-Vian, M.; Rakotomanomana, N.; Dangles, O. *J. Agric. Food Chem.* **2007**, *55*, 7573−7579.
(11) Yoshida, K.; Mori, M.; Kondo, T. *Nat. Prod. Rep.* **2009**, *26*, 884−915.
(12) Cruz, L.; Bras, N. F.; Teixeira, N.; Mateus, N.; Ramos, M. J.; Dangles, O.; De Freitas, V. *J. Agric. Food Chem.* **2010**, *58*, 3159−3166.
(13) Gonzalez-Manzano, S.; Duenas, M.; Rivas-Gonzalo, J. C.; Escribano-Bailon, M. T.; Santos-Buelga, C. *Food Chem.* **2009**, *114*, 649−656.
(14) Cruz, L.; Bras, N. F.; Teixeira, N.; Fernandes, A.; Mateus, N.; Ramos, M. J.; Rodriguez-Borges, J.; de Freitas, V. *J. Agric. Food Chem.* **2009**, *57*, 10341−10348.
(15) Nave, F.; Teixeira, N.; Mateus, N.; de Freitas, V. *Food Chem.* **2010**, *121*, 1129−1138.
(16) Pissarra, J.; Mateus, N.; Rivas-Gonzalo, J.; Buelga, C. S.; de Freitas, V. *J. Food Sci.* **2003**, *68*, 476−481.
(17) Geissman, T. A.; Yoshimura, N. N. *Tetrahedron Lett.* **1966**, *7*, 2669−2673.
(18) Brouillard, R.; Mazza, G.; Saad, Z.; Albrechtgary, A. M.; Cheminat, A. *J. Am. Chem. Soc.* **1989**, *111*, 2604−2610.
(19) Dangles, O.; Saito, N.; Brouillard, R. *J. Am. Chem. Soc.* **1993**, *115*, 3125−3132.
(20) Frisch, M. J. T., G. W.; Schlegel, H. B.; Scuseria, G. E.; Robb, M. A.; Cheeseman, J. R.; Scalmani, G.; Barone, V.; Mennucci, B.; et al. *Gaussian 09 (Revision A.1)*; Gaussian, Inc.: Wallingford, CT, 2009.
(21) Bayly, C. I.; Cieplak, P.; Cornell, W. D.; Kollman, P. A. *J. Phys. Chem.* **1993**, *97*, 10269−10280.
(22) Izaguirre, J. A.; Catarello, D. P.; Wozniak, J. M.; Skeel, R. D. *J. Chem. Phys.* **2001**, *114*, 2090−2098.
(23) Loncharich, R. J.; Brooks, B. R.; Pastor, R. W. *Biopolymers* **1992**, *32*, 523−535.
(24) Case, D. A., Darden, T. A., Cheatham, T. E., III; Simmerling, C. L., Wang, J., Duke, R. E., Luo, R., Crowley, M., Ross, C. W., Zhang, W., et al. AMBER 10; University of California: San Francisco, 2008.
(25) Cornell, W. D.; Cieplak, P.; Bayly, C. I.; Gould, I. R.; Merz, K. M.; Ferguson, D. M.; Spellmeyer, D. C.; Fox, T.; Caldwell, J. W.; Kollman, P. A. *J. Am. Chem. Soc.* **1995**, *117*, 5179−5197.
(26) Ryckaert, J. P.; Ciccotti, G.; Berendsen, H. J. C. *J. Comput. Chem.* **1977**, *23*, 327−341.
(27) Huo, S.; Massova, I.; Kollman, P. A. *J. Comput. Chem.* **2002**, *23*, 15−27.
(28) Kollman, P. A.; Massova, I.; Reyes, C.; Kuhn, B.; Huo, S. H.; Chong, L.; Lee, M.; Lee, T.; Duan, Y.; Wang, W. *Acc. Chem. Res.* **2000**, *33*, 889−897.
(29) Massova, I.; Kollman, P. A. *J. Am. Chem. Soc.* **1999**, *121*, 8133−8143.
(30) Massova, I.; Kollman, P. A. *Perspect. Drug Discovery Des.* **2000**, *18*, 113−135.
(31) Rocchia, W.; Alexov, E.; Honig, B. *J. Phys. Chem. B* **2001**, *105*, 6507−6514.
(32) Rocchia, W.; Sridharan, S.; Nicholls, A.; Alexov, E.; Chiabrera, A.; Honig, B. *J. Comput. Chem.* **2002**, *23*, 128−137.
(33) Allen, M. J.; Tozer, D. J. *J. Chem. Phys.* **2002**, *117*, 11113−11120.
(34) Brouillard, R.; Delaporte, B. *J. Am. Chem. Soc.* **1977**, *99*, 8461−8468.
(35) Hobza, P.; šponer, J.; Reschel, T. *J. Comput. Chem.* **1995**, *16*, 1315−1325.
(36) Kristyan, S.; Pulay, P. *Chem. Phys. Lett.* **1994**, *229*, 175−180.
(37) Malien-Aubert, C.; Dangles, O.; Amiot, M. J. *J. Agric. Food Chem.* **2002**, *50*, 3299−3305.
(38) Markovic, J. M. D.; Petranovic, N. A.; Baranac, J. M. *J. Agric. Food Chem.* **2000**, *48*, 5530−5536.
(39) Grimme, S. *J. Comput. Chem.* **2004**, *25*, 1463−1473.
(40) Grimme, S. *J. Comput. Chem.* **2006**, *27*, 1787−1799.
(41) Grimme, S.; Antony, J.; Ehrlich, S.; Krieg, H. *J. Chem. Phys.* **2010**, 132.
(42) Chai, J. D.; Head-Gordon, M. *J. Chem. Phys.* **2008**, 128.
(43) Di Meo, F.; Sancho Garcia, J. C.; Dangles, O.; Trouillas, P. *J. Chem. Theory Comput.* **2012**, *8*, 2034−2043.
(44) Houbiers, C.; Lima, J. C.; Macanita, A. L.; Santos, H. *J. Phys. Chem. B* **1998**, *102*, 3578−3585.
(45) Brouillard, R.; Dubois, J. E. *J. Am. Chem. Soc.* **1977**, *99*, 1359−1364.
(46) Dangles, O.; Brouillard, R. *Can. J. Chem.* **1992**, *70*, 2174−2189.
(47) Pina, F. *J. Photochem. Photobiol., A* **1998**, *117*, 51−59.
(48) Haslam, E. *Practical Polyphenolics—From Structure to Molecular Recognition and Physiological Action*; Cambridge University Press: Cambridge, 1998.